

Tracking Light-Induced Fragmentation of Single Silver Nanoparticles by Single Entity Electrochemistry

Mengjie Chen, Si-Min Lu*, Hao-Wei Wang, Yi-Tao Long*

(State Key Laboratory of Analytical Chemistry for Life Science, School of Chemistry and Chemical Engineering Nanjing University, Nanjing 210023, Jiangsu, P. R. China)

Abstract: Light irradiation on silver nanoparticles (Ag NPs) could cause the energy conversion, thus, the fragmentation of Ag NPs. It is important to detect the changes of fragmented Ag NPs in the aspects of physical and chemical properties. Herein, benefiting from the high sensitivity, high temporal resolution, and high-throughput, single entity electrochemistry (SEE) method is introduced to *in-situ* track the dynamic laser fragmentation of single Ag NP. Compared with UV-Vis absorption spectroscopy and transmission electron microscopy (TEM), SEE methods enables an accurate *in-situ* measurements of light-induced fragmentation of single Ag NP. The variation in the statistic current amplitude displays the real-time changes of single Ag NP upon laser irradiation for 60 min, which indicates that the laser of 532 nm wavelength is the most effective laser for the dynamic fragmentation. By virtue of the excellent sensing performance, SEE is further applied in revealing the heterogeneity in Ag NPs' intrinsic physicochemical properties, such as size, crystal structure, surface charge density. The study highlights the potential of SEE to advancing the real-time characterization of nanomaterials in the chemical reactions.

Key words: light-induced fragmentation; single entity electrochemistry; stochastic collision electrochemistry; single silver nanoparticles

1 Introduction

Single entity electrochemistry (SEE) is a rapidly growing research discipline opening up a broad range of potential applications in energy, chemistry, and cellular biology etc^[1-5]. SEE based on the collision of an entity with an ultramicroelectrode (UME) interface is defined as the stochastic collision electrochemical measurements^[6,7]. For a typical single entity stochastic collision measurement, an UME is immersed into a electrolyte solution containing a freely-diffusion of entities at a fixed electrode solutions polarization. By virtue of their Brownian motion, the single entities stochastically collide with the UME interface, caus-

ing discrete and high-throughput transient electrochemical responses that would be recorded by the high-bandwidth instrument^[8-12]. The characteristic properties of the ensemble entities could be obtained by statistically analyzing the high-throughput electrochemical signals^[11,12]. The studies based on the stochastic collision electrochemistry are important as it can not only detect the heterogeneity of entities itself, but also reveal the properties of entities (size, concentration, surface charge, and diffusion coefficient, etc.)^[13-17].

There has been considerable activity in the field of Ag NPs photochemical transformation in recent

Cite as: Chen M J, Lu S M, Wang H W, Long Y T. Tracking light-induced fragmentation of single silver nanoparticles by single entity electrochemistry. *J. Electrochem.*, 2022, 28(3): 2108521.

years, since Ag Nps has strong light absorption, thus allowing the wide applications in environmental chemistry, material science, and photophysics. Morphological/structure evolution and transformation mechanisms of Ag NPs in the light-induced fragmentation process are essential as crystal structure information underpin their physical and chemical properties^[18–20]. Therefore, it is extremely important to accurately characterize the Ag NPs changes induced by laser irradiation. To date, experimental insights on the structure characterization of Ag NPs have relied on transmission electron microscopy (TEM) and UV-Vis spectroscopy^[21]. The lack of straightforward and high-temporal resolution measurements, suitable to *in-situ* track the size or morphology change, is part of the reasons why the details of light-induced fragmentation of Ag NPs are still unclear. In addition, the surface property (surface charge density, surfactant, etc.) variation could not be directly revealed by the two characterization methods. Therefore, there is an urgent demand for a high sensitivity, high-temporal resolution and high-throughput measurement to monitor the dynamic light-induced fragmentation in real time.

SEE as a state-of-the-art electrochemistry technique has been applied to the study of multi-step electro-oxidation trajectories of individual Ag NPs^[22–26], where multiple distinct motion trajectories could be observed by the electro-oxidation of single Ag NP collision with the UME interface. Based on the theoretical predictions, the interaction-modulated dynamic electrochemical behaviors for the oxidation of single Ag NP have been investigated^[24,27]. Additionally, the electron transfer kinetics of single Ag NP electro-oxidation is explored by a Metal-Solution-Metal Nanoparticle (M-N-MNP) theoretical model that is proposed to reveal the dynamic “feeling” potential of a single Ag NP^[23]. By the advanced theoretical framework and electrochemical measurements, the size of individual Ag NPs could be calculated by the integrated charge of each time-resolved current response^[8]. Benefiting from the high sensitivity of SEE methods, herein, we demonstrate, in a proof-of-principle, that the use of stochastic collision electrochemistry as a

high-throughput and rapid method can be extended to the real-time monitoring of the dynamic light-induced fragmentation of Ag NPs. The light irradiation could cause the shrinkage of Ag NPs, thus, the decrease on the current amplitude and the increase in the collision frequency. Light irradiation with different wavelengths is further used to explore the light-induced fragmentation kinetics. The change of statistic current amplitude reveals that the most significant size variation of Ag NPs occurs after the laser irradiation at 532 nm, enabling the study of high-rate kinetic on the dynamic photolysis of Ag NPs.

2 Experimental Section

2.1 Reagents and Materials

Disodium hydrogen phosphate dodecahydrate ($\text{Na}_2\text{HPO}_4 \cdot 12\text{H}_2\text{O}$) and sodium dihydrogen phosphate dihydrate ($\text{NaH}_2\text{PO}_4 \cdot 2\text{H}_2\text{O}$) were purchased from Shanghai Aladdin Bio-Chem Technology Co., Ltd. Sulfuric acid (H_2SO_4 , 98.0wt%) was purchased from Nanjing Chemical Reagent Co., Ltd. Ag nanoparticles (30 nm, purity 99.99%) were purchased from NanoComposix Cooperation. Ultra-pure water ($18.2 \text{ } \Omega\text{m} \cdot \text{cm}$ at $25 \text{ } ^\circ\text{C}$) obtained from Sartorius arium®pro synthesis system was used to prepare stocking solution. Unless otherwise noted, all chemical reagents were used without further purification. Au UME (12.5 μm diameter, CHI105), saturated calomel electrode (SCE, CHI150), Pt wire electrode (CHI115) were purchased from Shanghai Chenhua Co., Ltd. Light source (365 nm ultraviolet light emitting diode, 5 W; a continuous-wave diode laser at 405 nm and 532 nm, 50 mW) was purchased from Guangzhou MTOLaser Co., Ltd, and was used for the light-induced fragmentation experiments.

2.2 Ag Nanoparticles Characterization

Transmission electron microscopic (TEM) images of Ag NPs were obtained on a JEM-2100 F (JEOL, Japan) transmission electron microscope at an acceleration voltage of 200 kV. Optical properties of the Ag NPs bulk solution were examined using a UV-Vis opticql spectrometer (Shimadzu UV-3600, Japan).

2.3 Au Ultramicroelectrode Cleaning

At first, the Au UME (12.5 μm diameter) was

cleaned via mechanical polishing in 0.05 μm alumina slurry, and ultrasonicated in ultra-pure water for 7 s. Cyclic voltammetric measurement in a 500 $\text{mmol} \cdot \text{L}^{-1}$ H_2SO_4 aqueous solution was performed to judge the surface status of the Au UME (leakage, cleanliness, electric double layer). (Detailed voltammograms are provided in the Supplementary Information Note 1). Cyclic voltammograms were recorded via a CHI852D electrochemical analyzer (CH. Instruments, Inc., Shanghai, China) in a traditional three-electrode system, including Au UME as the working electrode, saturated calomel electrode (SCE) as the reference electrode, and Pt wire as the counter electrode.

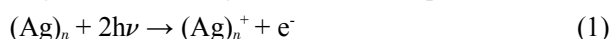
2.4 Electrochemical Measurements

Chronoamperometric experiments were performed on the low-noise current electrochemical instrument containing Axopatch 200B (Axon Instruments, Forest City, CA, USA) and DigiData PCI6281 (National Instruments, Austin, TX, USA) converter. The amplifier of internal low-pass Bessel filter was set as 5 kHz, and the data were acquired at a sampling rate of 100 kHz. The SEE test was performed with a two-electrode system in the 20.0 $\text{mmol} \cdot \text{L}^{-1}$ phosphate buffer (PB, pH 7.4) solutions containing 27.0 $\text{pmol} \cdot \text{L}^{-1}$ Ag NPs (30 nm diameter). The electrochemical cell consisted of a Au UME and an Ag/AgCl quasi-reference counter electrode (Ag/AgCl QRCE). All electrochemical measurements were performed in a Faraday cage at room temperature. The raw current data was further analyzed with the self-designed software (Py-nano, <https://github.com/deacenc/PyNano>).

3 Results and Discussion

To monitor the dynamic photoinduced fragmentation of single Ag NP, the stochastic collision electrochemistry test of individual Ag NPs at the Au UME was performed under the light irradiation. The raw i - t curves were obtained with the Au UME biased at +0.60 V vs. Ag/AgCl QRCE^[24], whether under the dark condition (Figure 1(A)) or visible light condition (Figure 1(B)), the electro-oxidation of 30 nm diameter Ag NPs in the tunneling region would cause a series of discrete spiky signals. Figure 1 and Figure S2 show that the current amplitude and integrated

charge of single transient signal under visible light significantly decrease compared with that in the dark conditions. We speculate that the light irradiation may result in the structure changes of Ag NPs as the current spike shape is closely correlated to the radius of Ag NPs^[24]. It has been reported that the light-induced fragmentation of Ag NPs follows the processes^[28]:



where $(\text{Ag})_n$ is the initial state of Ag NPs containing n Ag atoms, $(\text{Ag})_n^+$ is the transient state after $(\text{Ag})_n$ photoejection of an electron under light irradiation. Herein, a transient state of $(\text{Ag})_n^+$ formed *via* the photoejection of an electron with light irradiation, and then fragment into the small-sized Ag NPs^[29].

Ag NPs were proved to fragment into different sizes and shapes by different light wavelengths^[30,31]. We then investigated the effect of light wavelength on the fragmentation kinetics of Ag NPs. Figure 2 shows the statistic results of current amplitude and frequency of single transient oxidation current signals after the light irradiation, and a significant decrease on the current amplitude could be observed compared to the dark condition. On the contrary, the light irradiation leads to an increase in the collision frequency. In addition, there is almost no change in the

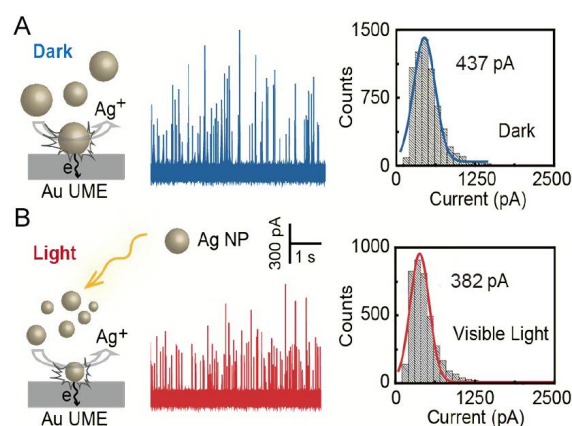


Figure 1 Schematic illustration, chronoamperometric i - t curves, and current amplitude histogram of electro-oxidation behaviors of single Ag NP collision with the Au UME interface under (A) dark and (B) visible light conditions (white light-emitting diode, light irradiation for 20 min). (color on line)

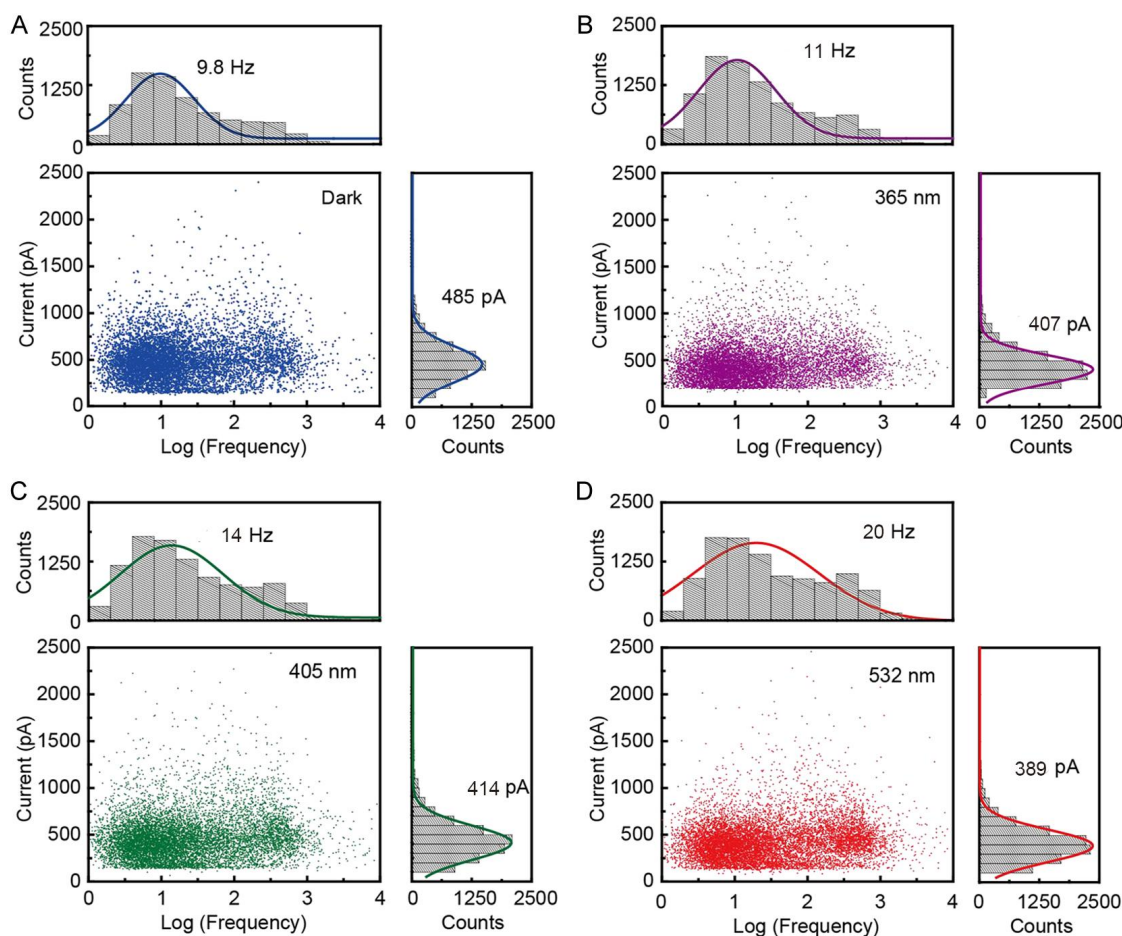


Figure 2 The histogram and scatter plots of current and frequency of transient oxidation current signals for single Ag NP collision with the Au UME interface after irradiation at different wavelengths of light: (A) Without light irradiation, (B) irradiation at 365 nm for 20 min, (C) irradiation at 405 nm for 20 min, (D) irradiation at 532 nm for 20 min. (color on line)

duration time of single current blips as illustrated in Figure S3. Compared with the light irradiations at 365 nm and 405 nm, the current amplitudes and integrated charges of single transient oxidation current signals could show significantly decrease after the laser irradiation at 532 nm. Therefore, laser irradiation at 532 nm was employed to investigate the dynamic light-induced fragmentation of single Ag NP *via* stochastic collision electrochemistry.

The effect of irradiation time on the dynamic light-induced fragmentation of Ag NPs was also tested for exploring the detailed photolysis kinetics of single Ag NP. As shown in Figure 3(A), the absorption spectra of Ag NPs after the light irradiation at 532 nm for different time could not display significant peak-shift. It is worth noting that the current am-

plitude of stochastic collision electrochemistry of single Ag NP decreases with the light irradiation (Figure S4 shows the statistic histograms of current amplitude of single Ag NP by SEE methods after different irradiation time). As depicted in Figure 3(B), plotting current amplitude versus irradiation time for various light wavelengths of 365, 405 and 532 nm yields linear plots with linear slopes of -1.8, -1.6 and -3.6, respectively. By comparing the slope value, 532 nm wavelength laser exhibits a significant effect on the light-induced morphology transformation of Ag NPs, indicating the most rapidly kinetics on the dynamic shrinkage of Ag NPs. It has also been reported that the laser of 532 nm wavelength is most effective for the fragmentation of Ag NPs^[28].

In the case of kinetics-limited electro-oxidation of

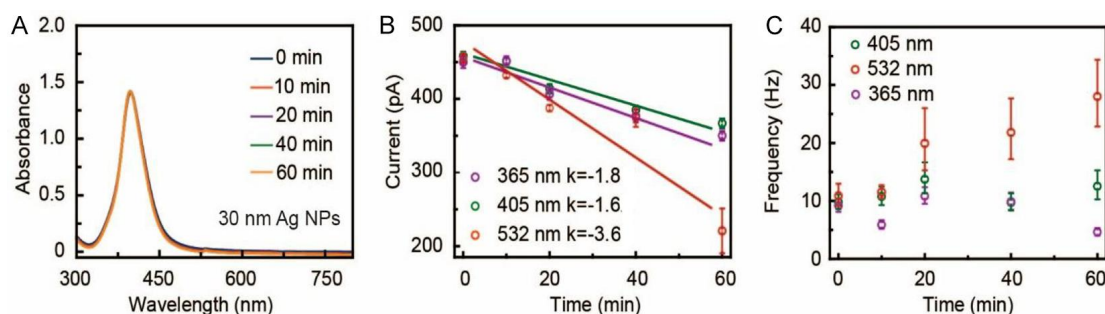


Figure 3 (A) The UV-Vis absorption spectra of Ag NPs irradiated under irradiation at 532 nm for different time. (B) A set of plots of current amplitude versus irradiation time for different irradiation wavelengths at 365 nm, 405 nm and 532 nm. (C) The changes in collision frequency of single Ag NP as a function of irradiation time for different irradiation wavelengths at 365 nm, 405 nm and 532 nm. (color on line)

Ag NPs, the current could be expressed as (a detailed derivation process is provided in the Supplementary Information Note 2)^[23]:

$$I = 4\pi k(r_{\text{NP}} - \frac{k}{\rho}t)^2 e \quad (4)$$

where k is the electrochemical oxidation dissolution rate constant of Ag NPs, r_{NP} is the initial radius of Ag NPs, t is the reaction time, e is the element charge. I is proportional to the radius of the Ag NPs, demonstrating that the extension of light irradiation time leads to the decrease in the radius of Ag NPs. Figure S5 and Table 1 show the histograms of integrated charge of Ag NPs after irradiation at different wavelengths of light. The statistic results of integrated charge of single transient blips are consistent with the change trend of the current amplitude after irradiation from 0 to 60 min, and the duration time of single transient signals is basically unchanged as illustrated in Figure S6. In addition, Figure 3(C) shows that the collision frequency of discrete transient blips changes with the irradiation time from 0 min to 60 min at different laser wavelengths. There is a significant increase in the collision frequency with the laser irradiation time at 532 nm. The collision frequency increases from 11 Hz to 28 Hz after 60 min irradiation (a detailed of the histograms of collision of discrete transient blips by SEE method after 532 nm laser irradiation at different irradiation time is showed in Figure S7). However, the light irradiations of 365 nm and 405 nm could barely not result in the obvious

change of collision frequency. At the most basic level, the collision frequency is closely correlated to the flux of Ag NPs to the Au UME. Under the conditions of steady-state flux of Ag NPs to the Au UME interface is given by the following equation^[32]:

$$J(t_0 \rightarrow t_1) = 4DC_{\text{NP}}r_d \quad (5)$$

where D is the diffusion coefficient of Ag NPs, C_{NP} is the concentration of Ag NPs, and r_d is the radius of Au UME. The Ag NPs diffusion coefficient can be estimated from the Stokes-Einstein equation as^[33]:

$$D = \frac{k_B T}{6\pi\eta r_{\text{NP}}} \quad (6)$$

where k_B is the Boltzmann constant, $T(\text{K})$ is the Kelvin temperature, and r_{NP} is the radius of Ag NPs. The diffusion coefficient of a Ag NPs is inversely proportional to its radius. Next, substitution of Eq. (6) into Eq. (5) gives:

$$J(t_0 \rightarrow t_1) = 4 \frac{k_B T}{6\pi\eta r_{\text{NP}}} C_{\text{NP}} r_d \quad (7)$$

Consequently, when the radius decreases, it could ultimately result in the increase in collision frequency. According to the above results, 532 nm wavelength irradiation leads to the exhibition of the most rapidly kinetics on the dynamic shrinkage of Ag NPs, hence the increases of collision frequency is the most obvious trend with the laser irradiation time at 532 nm. Table 1 shows the statistics of amplitude current and collision frequency of single Ag NP collision with the Au UME interface after irradiation at different wavelengths of light over time. It is worth noting that there

Table 1 The statistical results of collision frequency, current amplitude of transient current blips.*

Wavelength	Collision frequency (s ⁻¹)					Current amplitude (pA)					<i>k</i> ^d
	0 min	10 min	20 min	40 min	60 min	0 min	10 min	20 min	40 min	60 min	
365 nm ^a	9.2	5.9	11	10	4.6	450	452	407	377	350	-1.8
405 nm ^b	9.8	11	14	9.7	13	458	450	414	385	367	-1.6
532 nm ^c	11	12	20	22	28	456	432	388	374	221	-3.6

*The transient current blips by electro-oxidation of single Ag NP collision with the UME interface after light irradiations at different wavelengths from 0 to 60 min.

^a 365 nm ultraviolet light emitting diode (5 W).

^b A continuous-wave diode laser at 405 nm (50 mW).

^c A continuous-wave diode laser at 532 nm (50 mW).

^d Slope of linear plot of current amplitude versus irradiation time for various light wavelengths.

is no significant wavelength change in the UV-Vis spectrum under the laser irradiation at 532 nm from 0 min to 60 min, indicating that the ensemble information detected by UV-Vis concealed these heterogeneity and transient changes of Ag NPs in the dynamic photolysis process.

In order to determine the heterogeneity in the size of Ag NPs after light irradiation, the size distributions were obtained by SEE and TEM methods. By the size measurements based on SEE method, we estimate the Ag NPs size with the integrated charge of each oxidation current response by the following equation^[27]:

$$d = 2\sqrt[3]{\frac{3QM}{4\pi nF\rho}} \quad (8)$$

where *d* is the diameter of the Ag NPs, *Q* is the integrated charge from the transient oxidation current signals, *M* is the atomic molecule mass of Ag, *n* is the number of electrons transfer per Ag atom, *F* is Faraday's constant and *ρ* is the density of Ag. The diameter distribution of Ag NPs is obtained after irradiation at different wavelengths of light for 60 min (Figures 4 (A)-4(C)). As a comparison, Figures 4(D)-4(F) show the diameter distributions of Ag NPs characterized by TEM, and there are no obvious changes in the average size, morphology and dispersion of Ag NPs (the TEM characterization results are shown in Figure S8). It further demonstrates that the SEE method has ability to reveal the slight change in the dynamic

light-induced fragmentation process. Furthermore, the heterogeneity of Ag NPs is evaluated by the coefficient of variation (*C_v*) of size distribution based on the following equation:

$$C_v = \frac{\sigma}{\mu} \quad (9)$$

where *σ* is standard deviation of Ag NPs diameter, *μ* is the mean value of Ag NPs' diameter. A larger *C_v* would lead to a large degree of dispersion, thus showing more obvious heterogeneity of Ag NPs. Notably, a larger *C_v* was obtained by SEE method compared with that obtained by TEM (Figure 4). TEM characterization is a means for the direct detection of Ag NPs size. As for the SEE method, the volume of Ag NPs could be deduced by integrating the individual faradaic current responses that could be affected by the mass transport and electro-oxidation reaction kinetics of a single Ag NP at the Au UME interface. In addition to size, the intrinsic physical and chemical characteristics of Ag NPs including crystal structure and surface charge density would contribute to the variation in the current amplitude. Therefore, we speculate that the large *C_v* obtained by SEE method might represent a more fruitful physicochemical information of Ag NPs in the dynamic photolysis process. SEE method can reveal not only the heterogeneity in the size, but also the heterogeneity in other properties of Ag NPs, such as the crystal structure, the surface charge density and the dispersion state in

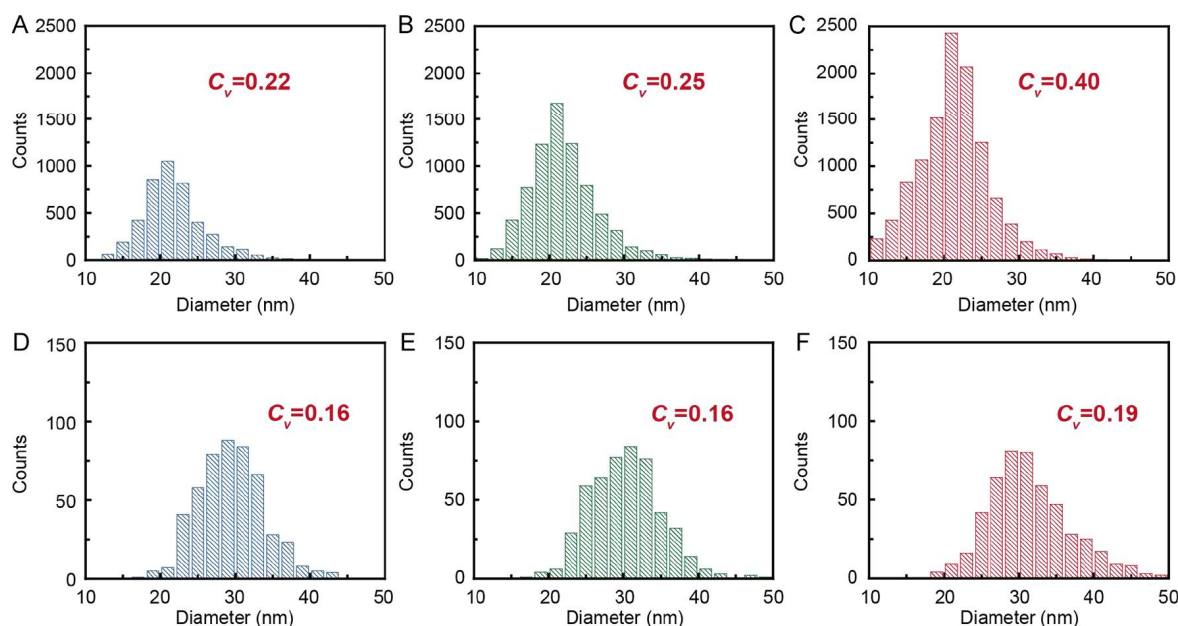


Figure 4 Diameter distributions of Ag NPs obtained *via* (A), (B), (C) by single entity electrochemistry method, and (D), (E), (F) by TEM characterization after irradiations at 365 nm, 405 nm and 532 nm for 60 min. C_v is the coefficient of variation of size distribution based on the standard deviation (σ) and the mean value (μ) of a Ag NP diameter. (color on line)

bulk solution.

4 Conclusions

In summary, we utilized SEE methods to detect the dynamic changes of Ag NPs during light-induced fragmentation. The laser irradiation lead to a decrease on the current amplitude of single transient blips and an increase in the collision frequency. Moreover, under the laser irradiation at 532 nm, the Ag NPs displayed the most obvious changes of current amplitude and integrated, indicating that the kinetics of shrinkage process is most rapid. In addition, high-throughput SEE methods accurately revealed the trival heterogeneity of Ag NPs. Our study indicates that SEE offers a versatile tool to deepen the understanding in the microscopic photolysis kinetics of nanomaterials at the nanoscale.

Acknowledgements:

This research is supported by the China Postdoctoral Science Foundation (2021M691506) and the National Natural Science Foundation of China (22090051, 22111530177). The authors thank Dr. Shao-Chuang Liu for the help of data processing.

References:

- [1] Wang Y X, Shan X N, Tao N J. Emerging tools for studying single entity electrochemistry[J]. *Faraday Discuss.*, 2016, 193: 9-39.
- [2] Crooks R M. Concluding remarks: single entity electrochemistry one step at a time[J]. *Faraday Discuss.*, 2016, 193: 533-547.
- [3] Baker L A. Perspective and prospectus on single-entity electrochemistry[J]. *J. Am. Chem. Soc.*, 2018, 140(46): 15549-15559.
- [4] Gooding J. Single entity electrochemistry progresses to cell counting[J]. *Angew. Chem. Int. Ed.*, 2016, 55(42): 12956-12958.
- [5] Lu S M, Peng Y Y, Ying Y L, Long Y T. Electrochemical sensing at a confined space[J]. *Anal. Chem.*, 2020, 92(8): 5621-5644.
- [6] Kwon S J, Zhou H J, Fan F R F, Vorobyev V, Zhang B, Bard A J. Stochastic electrochemistry with electrocatalytic nanoparticles at inert ultramicroelectrodes-theory and experiments[J]. *Phys. Chem. Chem. Phys.*, 2011, 13(12): 5394-5402.
- [7] Ren H, Edwards M A. Stochasticity in single-entity electrochemistry[J]. *Curr. Opin. Electrochem.*, 2021, 25: 100632.
- [8] Ma W, Ma H, Chen J F, Peng Y Y, Yang Z Y, Wang H F, Ying Y L, Tian H, Long Y T. Tracking motion trajectories of individual nanoparticles using time-resolved cur-

- rent traces[J]. *Chem. Sci.*, 2017, 8(3): 1854-1861.
- [9] Ustarroz J, Kang M, Bullions E, Unwin P R. Impact and oxidation of single silver nanoparticles at electrode surfaces: one shot versus multiple events[J]. *Chem. Sci.*, 2017, 8(3): 1841-1853.
- [10] Robinson D A, Liu Y W, Edwards M A, Vitti N J, Oja S M, Zhang B, White H S. Collision dynamics during the electrooxidation of individual silver nanoparticles[J]. *J. Am. Chem. Soc.*, 2017, 139(46): 16923-16931.
- [11] Peng Y Y, Ma H, Ma W, Long Y T, Tian H. Single-nanoparticle photoelectrochemistry at a nanoparticulate TiO₂-filmed ultramicroelectrode[J]. *Angew. Chem. Int. Ed.*, 2018, 57(14): 3758-3762.
- [12] Ma H, Ma W, Chen J F, Liu X Y, Peng Y Y, Yang Z Y, Tian H, Long Y T. Quantifying visible-light-induced electron transfer properties of single dye-sensitized ZnO entity for water splitting[J]. *J. Am. Chem. Soc.*, 2018, 140(15): 5272-5279.
- [13] Zhang J H, Zhou Y G. Single particle impact electrochemistry: analyses of nanoparticles and biomolecules[J]. *J. Electrochem.*, 2019, 25(3): 374-385.
- [14] Sun L L, Wang W, Chen H Y. Correlated optical imaging and electrochemical recording for studying single nanoparticle collisions[J]. *J. Electrochem.*, 2019, 25(3): 386-399.
- [15] Wang W, Su B F, Zhan D P. Preparation and characterization of prussian blue modified nanoelectrode[J]. *J. Electrochem.*, 2012, 18(3): 252-256.
- [16] Dick J E, Hilterbrand A T, Strawsine L M, Upton J W, Bard A J. Enzymatically enhanced collisions on ultramicroelectrodes for specific and rapid detection of individual viruses[J]. *Proc. Natl. Acad. Sci.*, 2016, 113(23): 6403-6408.
- [17] Xiang Z P, Deng H Q, Peljo P, Fu Z Y, Wang S L, Mandler D, Sun G Q, Liang Z X. Electrochemical dynamics of a single platinum nanoparticle collision event for the hydrogen evolution reaction[J]. *Angew. Chem. Int. Ed.*, 2018, 57(13): 3464-3468.
- [18] Tsuji T, Hashimoto S. Laser-induced fragmentation of colloidal nanoparticles[M]//Sugioka K (Editor). *Handbook of laser micro- and nano-engineering*. Springer, Cham. 2021: 1-20.
- [19] Hajiesmaeilbaigi F, Mohammadalipour A, Sabbaghzadeh J, Hoseinkhani S, Fallah H R. Preparation of silver nanoparticles by laser ablation and fragmentation in pure water[J]. *Laser Phys. Lett.*, 2006, 3(5): 252-256.
- [20] Hamad A H. Nanosecond laser generation of silver nanoparticles in ice water[J]. *Chem. Phys. Lett.*, 2020, 755(16): 137782.
- [21] Mika A P, Rousseau P, Domaracka A, Huber B A. Interaction of multiply charged ions with large free silver nanoparticles: multielectron capture, fragmentation, and sputtering phenomena[J]. *Phys. Rev. B*, 2019, 100(7): 075439-1-7.
- [22] Yu R J, Xu S W, Paul S, Ying Y L, Cui L F, Daiguji H, Hsu W L, Long Y T. Nanoconfined electrochemical sensing of single silver nanoparticles with a wireless nanopore electrode[J]. *ACS Sens*, 2021, 6(2): 335-339.
- [23] Lu S M, Chen J F, Peng Y Y, Ma W, Ma H, Wang H F, Hu P J, Long Y T. Understanding the dynamic potential distribution at the electrode interface by stochastic collision electrochemistry[J]. *J. Am. Chem. Soc.*, 2021, 143(32): 12428-12432.
- [24] Ma W, Ma H, Yang Z Y, Long Y T. Single Ag nanoparticle electro-oxidation: potential-dependent current traces and potential-independence electron transfer kinetic[J]. *J. Phys. Chem. Lett.*, 2018, 9(6): 1429-1433.
- [25] Kim J Y, Han D, Crouch G M, Kwon S R, Bohn P W. Capture of single silver nanoparticles in nanopore arrays detected by simulations amperometry and surface-enhanced raman scattering[J]. *Anal. Chem.*, 2019, 91(7): 4568-4576.
- [26] Li X T, Batchelor-McAuley C, Compton R G. Silver nanoparticle detection in real-world environments via particle impact electrochemistry[J]. *ACS Sens*, 2019, 4(2): 464-470.
- [27] Ma H, Chen J F, Wang H F, Hu P J, Ma W, Long Y T. Exploring dynamic interactions of single nanoparticles at interfaces for surface-confined electrochemical behavior and size measurement[J]. *Nat. Commun.*, 2020, 11: 2307.
- [28] Kamat P V, Flumiani M, Hartland G V. Picosecond dynamics of silver nanoclusters. photoejection of electrons and fragmentation[J]. *J. Phys. Chem. B*, 1998, 102(17): 3123-3128.
- [29] Eustis S, Krylova G, Eremenko A, Smirnova N, Schill A W, El-Sayed M. Growth and fragmentation of silver nanoparticles in their synthesis with a fs laser and CW light by photo-sensitization with benzophenone[J]. *Photochem. Photobiol. Sci.*, 2005, 4(1): 154-159.
- [30] Jin R C, Cao Y C, Hao E, Metranux G S, Schatz G C, Mirkin C A. Controlling anisotropic nanoparticle growth through plasmon excitation[J]. *Nature*, 2003, 425(6957): 487-490.
- [31] Mohanty J, Palit D K, Shastri L V, Sapre A V. Pulsed laser excitation of phosphate stabilised silver nanoparticles[J]. *J. Chem. Sci.*, 2000, 112(1) 63-72.
- [32] Park J H, Boika A, Park H S, Lee H C, Bard A J. Single collision events of conductive nanoparticles driven by

migration[J]. *J. Phys. Chem. C*, 2013, 117(13): 6651-6657.
[33] Ellison J, Batchelor-McAuley C, Tschulik K, Compton R G. The use cylindrical micro-wire electrodes for nano-im-

pact experiments: facilitating the sub-picomolar detection of single nanoparticles[J]. *Sens. Actuators B Chem.*, 2014, 200: 47-52.

单体电化学测量银纳米颗粒动态光解过程

陈梦洁, 芦思珉*, 王浩炜, 龙亿涛*

(南京大学化学化工学院, 生命分析化学国家重点实验室, 江苏 南京 210023)

摘要: 银纳米颗粒吸收光后会发​​生能量转换从而导致其晶体结构变化, 分析光解过程中纳米颗粒的物理和化学性质十分重要。本文利用具有高灵敏度、高时间分辨率和高通量性质的单体电化学测量技术, 原位实时追踪单个银纳米颗粒的动态光解过程。当银纳米颗粒与限域电极界面碰撞时, 其会发生动态氧化, 从而产生高通量的法拉第电流信号。激光照射会使银纳米颗粒结构发生变化, 导致瞬态电流幅值降低和碰撞频率升高。通过统计高通量计时电流信号, 实现了对银纳米颗粒在光照条件下的形貌和结构转变过程的定量评估。研究表明, 单体电化学可精准获取光解过程中银纳米颗粒的结构变化信息, 揭示颗粒之间物理化学性能的异质性, 有助于在单颗粒尺度上对银光解动力学进行深入探究。

关键词: 光解; 单体电化学; 随机碰撞电化学; 银纳米颗粒